Cooperative Grid-Forming Control Strategy for PV and Battery Energy Storage System in an Isolated Microgrid.

M. FARRAJ, R. KALUTHANTHRIGE, A.D. RAJAPAKSE
University of Manitoba, Solar Solution
Canada

SUMMARY

Locally available solar PV energy alongside energy storage has emerged as a feasible renewable retrofit to the solely diesel-based remote off-grid power systems. In such areas, the grid-forming task is usually assigned to a dispatchable source such as a battery energy storage system (BESS), while the PV inverter operates as a grid-feeding unit due to the intermittent nature of PV power. The BESS unit, however, has a limited amount of energy and might sometimes fail to attain the preassigned voltage and frequency of the microgrid. Therefore, the capability of PV inverter to support the BESS unit in the grid-forming task in the absence of a diesel-based synchronous generator is critical when trying to reduce, optimize or replace the carbon-dependent generation capacity.

The intermittent nature of PV power imposes many constraints on operating the PV inverter as a gird supporting inverter while extracting the maximum available PV power. The operation of PV along BESS as grid-supporting inverter is governed under droop strategy to achieve load-sharing. However, this leads to inefficient sharing of energy between the BESS and the PV system, as the PV would operate at lower level than its maximum power level.

This paper outlines the control and operation of PV and BESS under grid-feeding and grid-forming modes applicable for isolated systems. It also presents an adaptive droop strategy for low voltage microgrids to achieve efficient parallel operation of PV and battery as grid forming inverters. The presented strategy facilitates maximum power point tracking (MPPT) operation and active power curtailment of PV to manage different operational scenarios by charging and discharging the battery. The simulation model of the considered isolated power system was built in the RTDS real-time simulation platform.

KEYWORDS

Renewable integration, Solar PV, Droop control, Grid-forming, Grid-following

farrajm@myumanitoba.ca

1   Introduction

Locally, available solar Photovoltaic (PV) power has become a rational renewable addition to the primarily fossil-fuel based remote power systems [1]–[3]. The modular nature of PV enables gradual expansion making investments manageable and avoiding idle capacity. Due to the intermittency of solar radiation, PV power generation is often classified as non-dispatchable [4]. Therefore, when considering isolated distribution networks, PV units are often integrated in a hybrid configuration alongside a dispatchable Distributed Generator (DG) or a Distributed Storage (DS) unit. PV-Diesel-Battery Hybrid Renewable Energy System (HRES) topology at high PV penetration levels is emerging as a reliable and cost-effective solution to remote off-grid power systems [2]. In such power systems for periods with high renewable power generation, economic dispatch models show that it is economical to meet the load demand and reserve requirements solely by the inverter-interfaced PV and battery units without any synchronous generator (isolated mode) [5]. During such scenarios, either PV or battery unit must form the grid, what can be very challenging considering the conditions prevailing in these remote power systems, especially at a 100% instantaneous Non-Synchronous Generation (NSG) penetration level.

It is desirable to regulate the output power of a non-dispatchable generation unit, such as a PV array, in a way to extract the maximum available power [4]. Thus the PV operation is usually governed under the grid-noninteractive Maximum Power Point Tracking (MPPT) mode while the dispatchable storage unit performs the grid-forming task [4]. However, extreme weather scenarios, changes in power system conditions, and sudden power fluctuations could impose constraints on system conditions such as physical limitations of the storage unit, operating reserve requirements, and regulation of reactive power output, which had not been anticipated by the adopted supervisory-level controls. Therefore, capability of the PV unit to operate in different operating modes to curtail active power, limit power fluctuations, and provide reactive power support becomes more significant under such conditions.

The deployment of PV units in the grid-forming task either solely or jointly with other sources is not considered as an optimum option due to the associated intermittency and uncertainty of its primary energy source [4]. Yet the capability of the PV array in forming the grid would strengthen the control redundancy of the remote off-grid systems in the absence of a synchronous generator. Especially if the storage unit fails during the isolated mode of control, the back-up diesel generator is responsible of taking over the grid-forming task. However, under low loading conditions with excess of renewable energy, diesel generator will have to be operated at part-loading events that could adversely affect its lifetime and operational efficiency [1], [5]. Thus, PV unit's capability to support the grid-forming task can be considered as an asset especially in context of remote off-grid power systems. Also, accurate prediction of the available solar power is required to operate the PV unit under the grid-forming mode as discussed in [6].

Most of the existing literature discussing PV control strategies such as MPPT mode, ramp-rate limitations [7], [8], power curtailment [1], [8], and frequency droop functions [8] are formulated for PV-units either connected to a stiff utility grid or the ones operating synchronized to a conventional generator. A limited number of studies focus on the grid-forming PV units under isolated mode [9], [10]. Therefore, a generic assessment of PV unit controls under isolated mode for both grid-following and grid-forming control is warranted. Such analysis would enhance the understanding of control strategies subjecting isolated PV units operated in the absence of synchronous generation and address the dearth of research in this specific area. This paper presents control strategies for operating a PV unit in an isolated hybrid PV-Battery configuration under both grid-feeding and grid-forming strategies. It also proposes an adaptive joint grid forming strategy of PV-Battery while controlling/maximizing the PV unit power. The results are demonstrated in the RTDS™ real-time simulation environment.

2   TEST SYSTEM SET-UP

As shown in Fig. 1, the considered renewable energy system operating in isolated mode consists of a Li-ion Battery Energy Storage System (BEES) with a DC rating of 600 kW, 912 kWh along with a 600 kW PV array [2]. The PV unit is connected to its VSC DC bus through a boost converter controlled to facilitate different control modes. While BESS is linked to its VSC DC bus using a bidirectional buck/boost converter to regulate the VSC DC bus voltage and supervise charging/discharging modes.

Both PV and BESS units are interfaced to the AC network through a Voltage Source Converter (VSC) governed under the carrier-based Pulse Width Modulation (PWM) technique. An LCL filter connected at the output of each VSC is also deployed to mitigate the effect of switching harmonics of the converters. The power system operation was modeled in the Real-Time Digital Simulator (RTDS) simulation environment while appropriately configuring the in-built PV, battery, and load models. The PWM converters were modelled as average models to reduce the computational power required, whereas the main concern is the dynamic behaviour of the system that presents low pass attributes. Therefore, the VSC is represented via a dependent DC current source along with three dependent voltage sources [11] and the DC-DC converters were modelled using average circuit topology, in which dependent voltage and current sources are used to interpret the diode and switching behaviour [12].
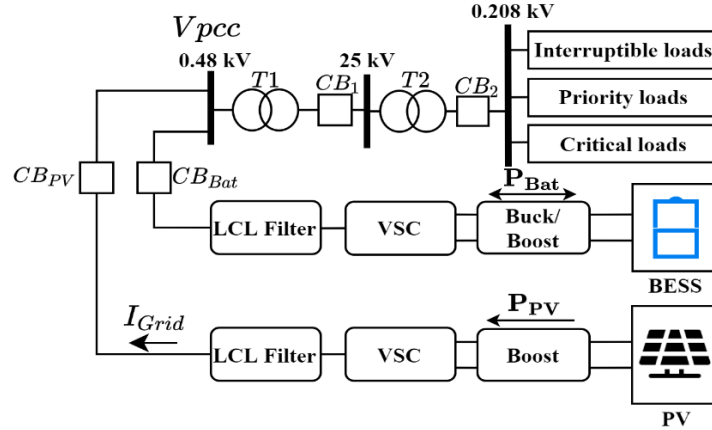

Figure 1 – Battery-PV isolated system configuration

3   CONTROLLER DESIGN OF PV UNIT

3.1   PV-VSC Controller

According to Fig. 2, a three-phase current feed-forward control strategy in the d-q rotating frame was adopted to govern the VSCs. The three-phase current and voltage quantities were transformed into DC quantities in the d-q frame by the means of Park transformation. The d-q axis current components (i_d^{VSC}, i_q^{VSC}) were independently regulated with its respective reference commands (i_d^{Ref}, i_q^{Ref}), which are generated by an outer voltage or power control loop.
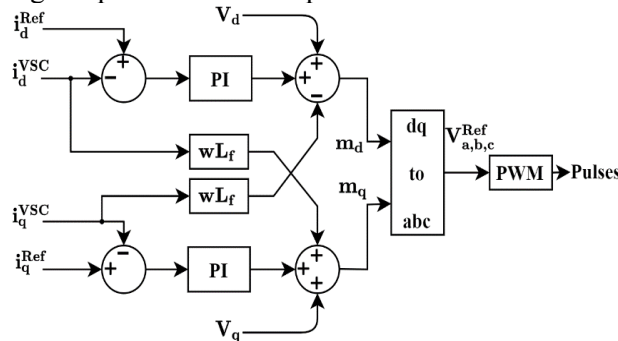

Figure 2 – Inner current control loops

3.1.1   Grid-feeding control

Grid-feeding control strategy is usually assigned to non-dispatchable resources such as PV and wind. Such inverters operate as current controlled sources that export pre-defined active and reactive power amounts to the AC grid formed by a grid-forming controller [13]. A key function of stable operation for PV-VSC is the regulation of the DC-link voltage to control/maximize the output power of the PV unit [14]. Fig. 3 shows the control blocks for this strategy, in which the d-q axis current references (i_d^{Ref}, i_q^{Ref}) were derived to regulate the DC link voltage (V_{DC}) and reactive power output (Q_{VSC}) at their desired references, respectively. The DC-link voltage reference (V_{DC}^{Ref}) is set to 1.1 kV and is regulated by balancing the power flow-in and flow-out of the DC-link. Unless specified otherwise, the Qref is set

to zero to achieve a unity power factor operation. A Phase locked loop (PLL) is also utilized to synchronize the PV-VSC reference signals with the AC grid formed by the BESS.
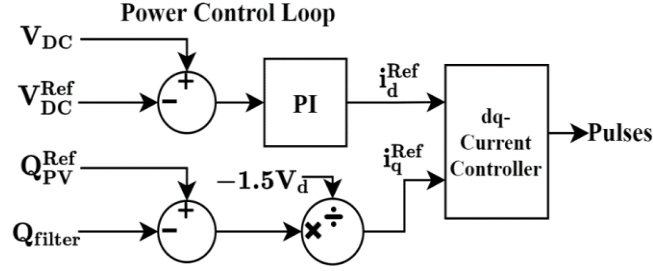

Figure 3 - PV-VSC power control loop.

3.1.2 Adaptive grid-forming control

The BESS sometimes has a limited amount of energy and might fail to attain the required voltage and frequency assigned by the grid operator. So, the capability of operating the PV unit as a grid-supporting inverter[13] can be crucial to maintain stable and reliable operation in such remote areas. Under this strategy, the PV and BESS are assigned to jointly form the grid. The operation of BESS and PV as grid forming sources connected in parallel can be realized by deploying a droop strategy. However, this would impose a constraint on extracting the freely available maximum power of the PV array as the PV-VSC output is driven by AC grid conditions. So, in the long run, it would be inefficient in contrast to the operation discussed in Section 3.1.1.

The derivation of inner-current control loop references (I_d^{Ref}, I_q^{Ref}) were modified using two outer-voltage control loops as shown in Fig. 4, where C_f is the AC side filter capacitance and K_d is the current feed-forward coefficient[15]. In d-q framework, by giving $V_q^{Ref} = 0$, the d-axis is oriented with the voltage vector. So, the regulation of Vd is adequate in controlling the AC voltage magnitude at the required reference (V_d^{Ref}) [15]. The outer d-q axes voltage control loops to regulate (V_d, V_q) at its corresponding references (V_d^{Ref}, V_q^{Ref}) are shown in Fig. 4(b) & (c). The incorporation of the feed-forward signals, $C_f w V_q$ and $C_f w V_d$ is expected to reduce the coupling effects on the outer-voltage control [16]. In addition, d-q components of the VSC grid-side current (I_d^{Grid}, I_q^{Grid}) were also incorporated to mitigate the effects of load dynamics on the voltage control task[16].
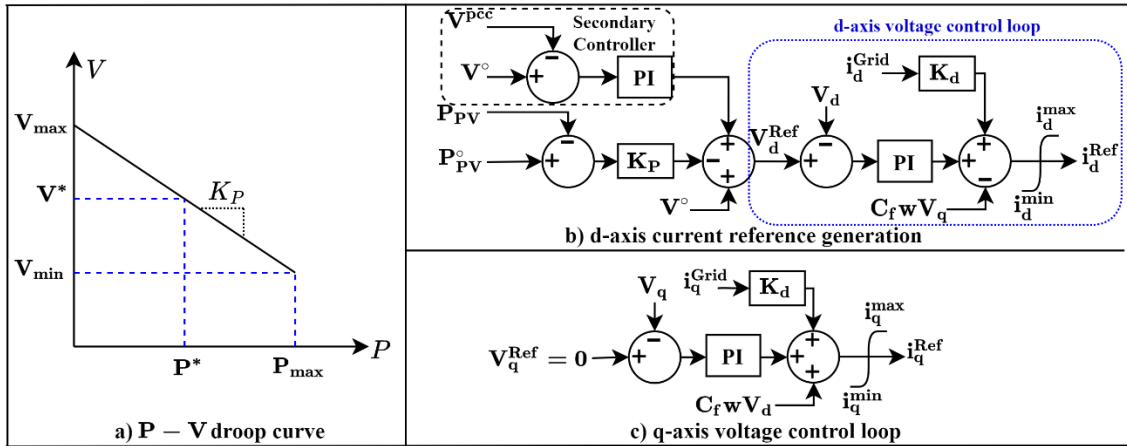

Figure 4 - PV-VSC voltage control loops.

In remote MV/LV power systems, the grid impedance is mainly resistive. Therefore, in contrast to the $P - f$ and $Q - V$ droop curves used in conventional power systems, $P - V$ and $Q - w$ droop curves were formulated as illustrated in Figs. 4(a) and 5(a) for the PV and BESS operating in grid forming mode. These $P - V$ and $Q - w$ droop curves can be mathematically expressed as in (3) and (4) [17]:

$$V = V° - K_P(P° - P) \tag{3}$$
$$w = w° + K_Q(Q - Q°) \tag{4}$$

where V and w represent the voltage and angular frequency outputs of the droop curves, respectively; K_P and K_Q are the real and reactive powers droop coefficients; P° and Q° are the active and reactive

3

powers set points and V° and w° are the nominal voltage and frequency values of the grid, respectively. The d-axis voltage reference (V_d^{Ref}) and the frequency reference (w^{Ref}) for the VSC were derived from (3) & (4), respectively. The droop curves produce a deviation in the voltage and frequency of the VSC as a function of the real and reactive powers (P, Q) delivered to the grid. Thus, a secondary restoration controller to restore the nominal voltage and frequency of the VSC was implemented. In islanded mode, the frequency (w^{Ref}) is controlled in an open-loop manner using an oscillator at a fixed frequency (w^{Ref}) [13], [15]. The rated frequency (w°) is provided as a feed-forward term to enhance the dynamic response of the oscillator. Fig. 4(a) & (b) and Fig. 5 depict the external droop control loops schemes. Similar outer voltage and droop control loops were implemented in the battery-VSC.

a) $\mathbf{Q - w}$ droop curve
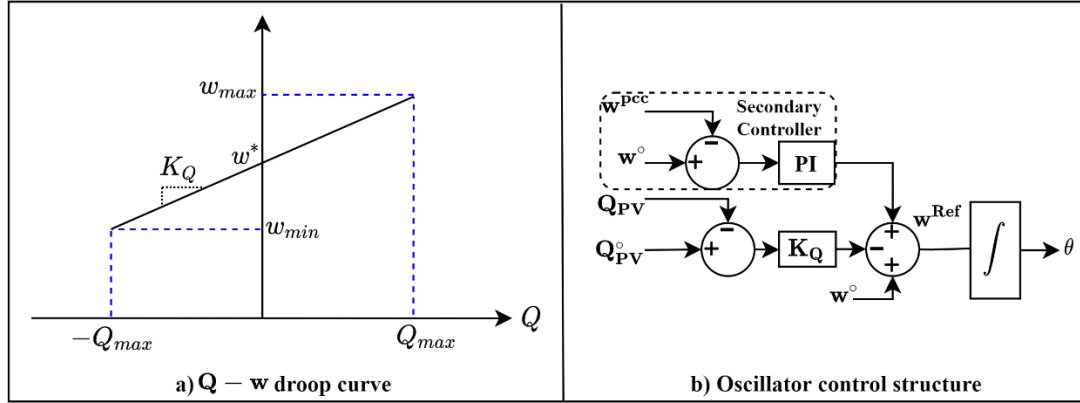
b) Oscillator control structure

Figure 5 – Frequency external control loop.

The droop strategy is used to achieve power-sharing between VSCs. However, when a PV-VSC is participating in the droop control, it would be inefficient as the main concern is to harness the available maximum PV power. Also, the stability of the system might get compromised if PV-VSC couldn't satisfy the power requirement assigned by the droop curves. To operate the PV-VSC as a grid-forming source, the PV array should operate at a lower level than its maximum available power, such that the reserved power facilitates forming of the voltage and frequency[6]. To achieve this, an adaptive PV power set point ($P_{PV}°$) for the $P - V$ droop is introduced that changes continuously to ensure coordinated and effective operation of the PV-VSC along battery-VSC. Two different modes to derive $P_{PV}°$ were implemented: reserve mode and load-following mode. During reserve mode, The PV unit is pushed to operate near MPPT with adequate reserve, which is very crucial for PV grid-forming inverter. This can be obtained by comparing a scaled MPPT PV voltage reference (V_{MPPT}) with PV array voltage (V_{PV}) to generate an error signal. The error signal is then passed to a PI controller in order to generate the setpoint $P_{PV}°$. As it is recommended in reserve mode to operate the PV array at a voltage that is higher than V_{MPPT} [6], the reserve coefficient is set higher than one ($K_{MPPT} > 1$). In load-following mode, this mode is enabled only when both SOC goes above its maximum value (SOC_{max}) and PV real power (P_{PV}) is higher or equal than the load power (P_L). Under this mode, P_{PV} is compared with P_L to generate an error signal that is then passed to a PI controller. In the proposed adaptive setpoint, the two modes are switched continuously to provide an effective response for sudden variations in load and solar irradiance. Fig. 6 shows the control blocks of $P_{PV}°$ generator.
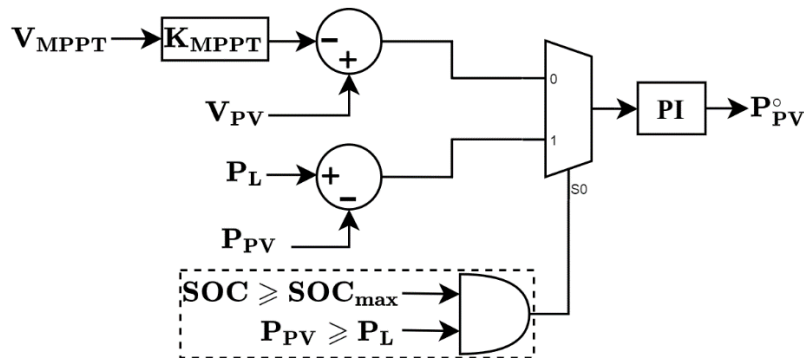

Figure 6 - PV-VSC power reference generator schematic.

3.2 PV boost controller

To extract the freely available maximum power at each operating condition, Maximum Power Point Tracking (MPPT) algorithms were developed in the literature. In this model, a technique called fractional open circuit voltage was used, which gives a voltage reference of the PV array to be tracked by the boost converter in order to utilize the maximum available power. Based on the control strategy used for PV-VSC and BESS SOC, the PV array controlling approach is varied. Three different techniques are devised namely: MPPT control, limited-power control, and DC-link voltage control. For example, during periods with excess renewable energy, the active power output of the PV unit must be restricted as specified by the supervisory controller. The amount of power curtailed will depend on the event that triggered this mode. For the isolated mode of operation, the PV power curtailment is usually triggered by battery overcharge scenarios. If the grid-forming battery unit reaches its overcharge boundary due to a sustained energy surplus period, the supervisory controller initiates the power curtailment mode (Limited-power = 1 and Grid-forming = 0). During this mode, the solar PV array's reference power is determined by the supervisory controller, and the PV voltage will fall between the maximum and open circuit voltage. In MPPT mode (Limited power =0 and Grid-forming = 0), the MPPT voltage reference is tracked by the boost converter to harness the maximum available power. In islanded mode (Grid-forming = 1), the boost converter was controlled to maintain the DC-link voltage at its desired reference. Note that, (Limited-power = 1 and Grid-forming = 1) is not an acceptable option. Fig. 7 demonstrates the control block of the boost converter.
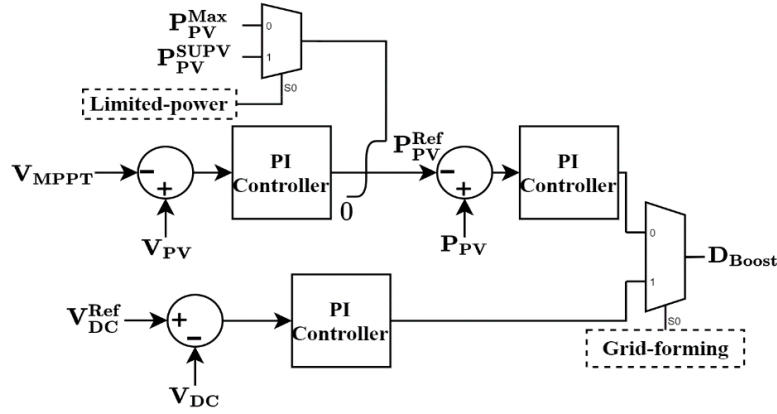

Figure 7 – PV array controller.

4 RESULTS AND DISCUSSION

The detailed control strategies were simulated on the RTDS™ real-time simulation environment for the hybrid PV-Battery configuration depicted in Fig. 1. The results obtained under the grid-following and grid-forming modes are discussed in the following sub-sections.

4.1 Grid-feeding

As discussed in Section 3.1.1, under the grid-following mode, PV unit operates as a current source synchronized to the AC grid formed and regulated by the battery unit controls. In the scenario showcased in Fig. 8, the hybrid power system is initially supplying a load of 0.3 MW at a unity PF. The PV unit active power output is following the commanded reference value for an irradiance level of 100 W/m². Also, the PV reactive power output is regulated at zero. Due to the lower PV power availability, battery-unit supplies most of the required active power to balance the grid. Also, the reactive power requirement of the lines and transformers are supplied by the battery unit at a value of 0.06 MVAR.

Starting from 15s irradiance gradually increases and settles at 800 W/m2. The MPPT controller changes the PV power reference to harness the maximum available power, and the PV output closely follows this reference. When the PV power output exceeds the load demand, the battery unit balances the active power by moving its operation into the charging mode. The PV active power reference reduces following a gradual irradiance reduction initiated at 23s. The PV output settles in a new steady state condition at 0.19 MW and the battery-VSC provides the required active power slack. Starting at 28s, a load change takes place, increasing both active and reactive power demand. The battery unit increases its output

power to balance the modified load demand while the PV unit continues its operation in the MPPT mode at a unity power factor. In all demonstrated system changes, the frequency and AC voltage variations showcase a stable response. The PV DC-link response depicts a slight change from its nominal value of 1.1 kV during the periods of irradiance change due to the MPPT tracking control imposed at the PV output voltage. However, once the irradiance settles, the DC-link voltage gets closely regulated at its nominal value.
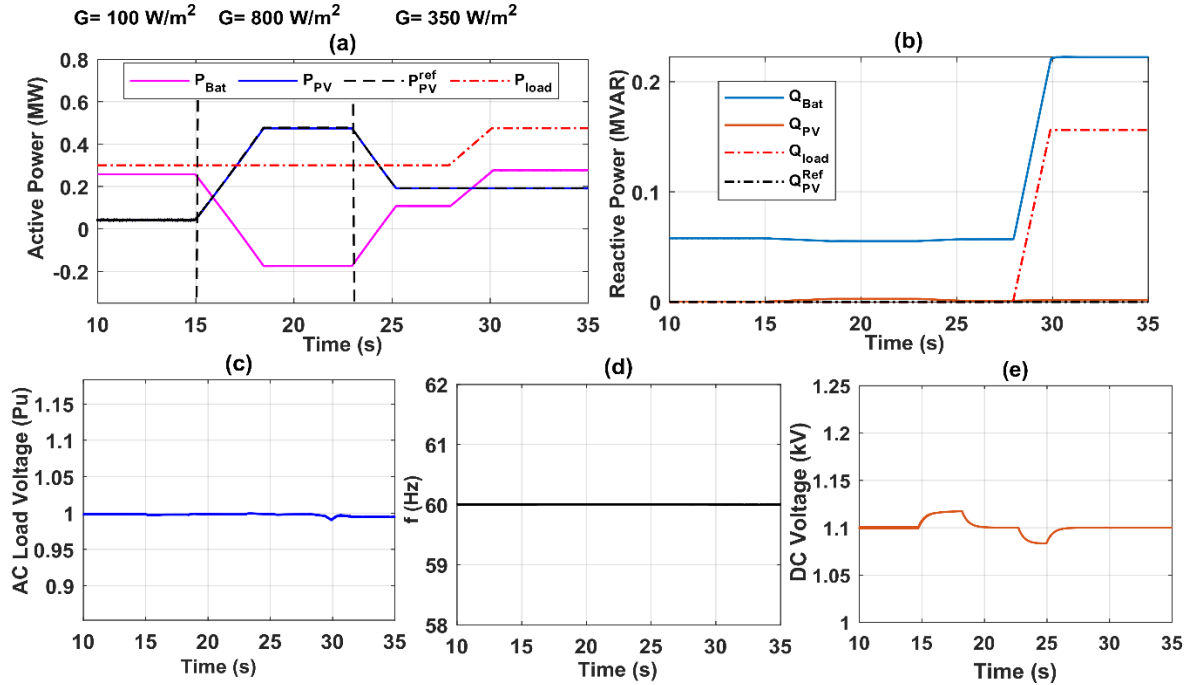

Figure 8 – Grid-feeding operating mode (a) active power (b) reactive power (c) AC voltage (d) frequency (e) PV DC-link voltage

4.2 Adaptive grid-forming

In this mode, the PV and BESS were equipped with grid-forming functions governed by external droop control loops. The PV unit was configured to operate near MPPT with adequate reserve under normal conditions and to take over the load-balancing task in the event of a battery unit failure. Fig. 9 depicts a scenario where both units are contributing to the grid-forming task. Initially, the system is supplying a load close to 0.4 MW at unity PF. PV-VSC active power is regulated at the maximum power value corresponding to an irradiation level of 500 W/m^2. The battery-VSC is supplying the remaining active power at a power level close to 0.13 MW. The reactive power requirement of the lines and transformers is shared between the battery and PV VSCs as shown in Fig. 9(b).

Around 15s, the load increases to a value of 0.5 MW. PV-VSC continues its operation providing the maximum power and the battery-VSC increases its active power to balance the grid. The irradiance starts to increase around 20s and settles at a value of 1000 W/m^2. Battery moves into the charging mode to balance the grid by absorbing the excess energy. Under all simulated system changes the reactive power outputs from the two VSCs showcase a stable response. Also, the AC voltage, DC-link voltage and the system frequency is maintained at their nominal values. The battery unit fails close to 25s and the PV-VSC moves away from its MPPT operation and starts to solely form the grid while balancing the active and reactive power. The sudden change of controls initiates a small transient period, and the system recovers to a steady state within 0.4s time. At 30s, the load starts to decrease and settles at 0.3 MW. The PV-VSC reduces its output power according to the updated grid conditions and the system runs smoothly.

Figure 10 depicts the response of control imposed under limited power mode. Initially, the PV output is controlled around 0.45 MW under MPPT control, and the battery unit supplies the balance of power operating in the discharging mode. Around 14s, the battery reaches its upper SOC limit (SOC$_{max}$), which is defined to be 90% in this case as shown in Fig. 10(b). The supervisory controller anticipates an overcharging scenario and initiates the PV limited-power mode to shift the grid-forming battery into

6

idle state as detailed in section 3.1.2. Around 19s, The PV output power increases following a load increase keeping the battery at an idle state. A load change starting at 28s increases the active power demand. The battery unit starts discharging while the PV unit shifts to MPPT control mode. Close to 38s, the irradiance starts to decrease and settles at a value of 500W/m^2. This change reduces the PV active output power while the battery active output power shifts upward to balance the load demand. As shown in Fig. 10(a) and (b), this allows the battery and PV units to jointly form the gird while avoiding overcharging scenario.
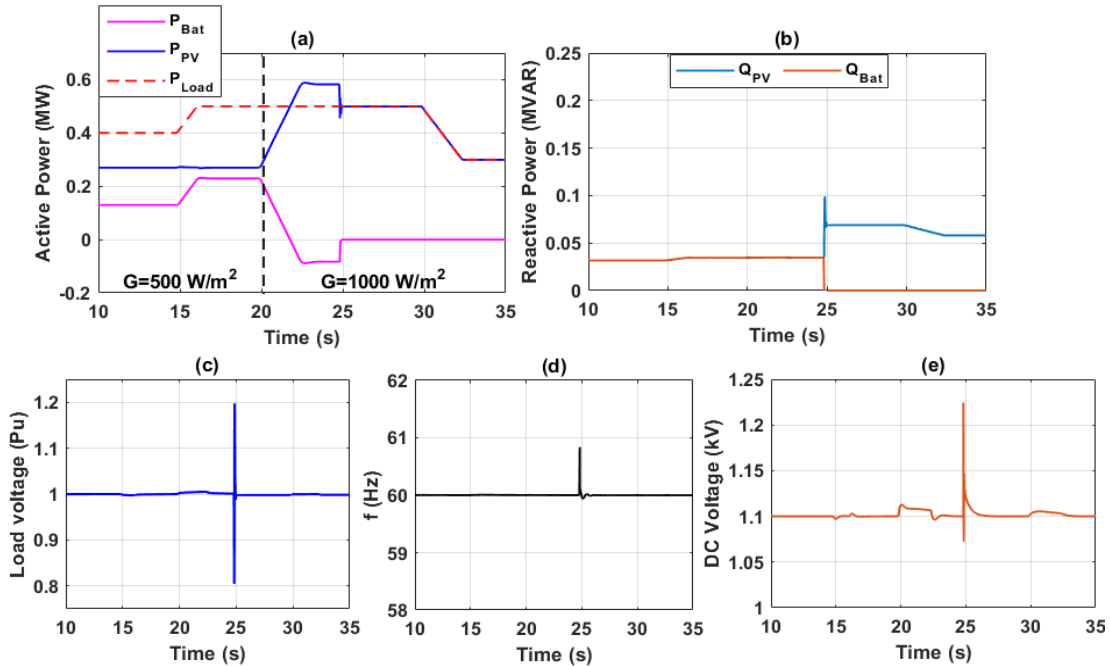

Figure 9 – Grid-forming operating mode (a) active power (b) reactive power (c) AC voltage (d) frequency (e) PV DC-link voltage
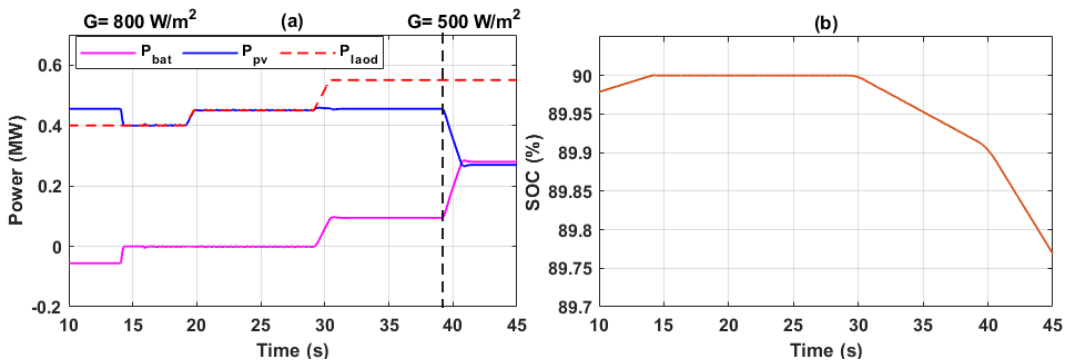

Figure 10 – Grid-forming operating mode (a) active power (b) battery SOC

5   CONCLUSION

As many remote off-grid power systems are attempting to achieve a carbon-free energy mix, competence of the PV controls to support critical grid forming functions becomes essential for operating with zero synchronous inertia over prolong periods. This paper presents and discusses several control strategies for a PV unit in a hybrid PV-Battery grid topology during an isolated mode of control. Both PV grid-feeding and grid-forming controls are investigated under load changes, solar irradiance changes, power curtailment modes, and component failures. When the battery-VSC operates as the slack bus, the PV-unit governed under the grid-following controls perform well in achieving the expected output conditions under all considered operating modes. The results also confirm the capability of PV unit to operate under the grid-forming controls while maximizing the penetration of freely available solar energy. In conclusion, the competence of the PV-VSC to operate under several modes adds to the control capability of the overall power system while bolstering the reliability and availability of power supply.

7

BIBLIOGRAPHY

[1]   R. Tonkoski, L. A. C. Lopes, and D. Turcotte, "Active power curtailment of PV inverters in diesel hybrid mini-grids," *2009 IEEE Electr. Power Energy Conf. EPEC 2009*, pp. 1–6, 2009, doi: 10.1109/EPEC.2009.5420964.

[2]   R. Kaluthanthrige, A. D. Rajapakse, C. Lamothe, and F. Mosallat, "Optimal Sizing and Performance Evaluation of a Hybrid Renewable Energy System for an Off-Grid Power System in Northern Canada," *Technol. Econ. Smart Grids Sustain. Energy*, vol. 4, no. 1, pp. 24–26, 2019, doi: 10.1007/s40866-019-0061-5.

[3]   A. Yazdani *et al.*, "Modeling guidelines and a benchmark for power system simulation studies of three-phase single-stage photovoltaic systems," *IEEE Trans. Power Deliv.*, vol. 26, no. 2, pp. 1247–1264, 2011, doi: 10.1109/TPWRD.2010.2084599.

[4]   A. D. F. Katiraei, R. Iravani, N. Hatziargyriou, "Microgrids Mamagement," *katiraei, Farid Iravani, Reza Hatziargyriou, Nikos Dimeas, Aris*, no. june, pp. 54–65, 2008.

[5]   R. Kaluthanthrige and A. D. Rajapakse, "Operational Optimization of a Remote Off-Grid Hybrid Renewable Energy System in Northern Canada," *2019 IEEE 7th Int. Conf. Smart Energy Grid Eng.*, pp. 268–273, 2019, doi: 10.1109/sege.2019.8859885.

[6]   Z. Chen, R. H. Lasseter, and T. M. Jahns, "Active power reserve control for grid-forming PV sources in microgrids using model-based maximum power point estimation," *2019 IEEE Energy Convers. Congr. Expo. ECCE 2019*, pp. 41–48, 2019, doi: 10.1109/ECCE.2019.8913174.

[7]   B. I. Crăciun, T. Kerekes, D. Séra, R. Teodorescu, and U. D. Annakkage, "Power Ramp Limitation Capabilities of Large PV Power Plants With Active Power Reserves," *IEEE Trans. Sustain. Energy*, vol. 8, no. 2, pp. 573–581, 2017, doi: 10.1109/TSTE.2016.2612121.

[8]   E. Bullich-Massagué, M. Aragüés-Peñalba, A. Sumper, and O. Boix-Aragones, "Active power control in a hybrid PV-storage power plant for frequency support," *Sol. Energy*, vol. 144, pp. 49–62, 2017, doi: 10.1016/j.solener.2016.12.033.

[9]   Z. Chen, R. H. Lasseter, and T. M. Jahns, "Power Reserve for Grid-Forming PV Sources with Stability Enhancement in Mixed-Source Microgrids," *IEEE Power Energy Soc. Gen. Meet.*, vol. 2019-Augus, 2019, doi: 10.1109/PESGM40551.2019.8973672.

[10]   Z. Chen, D. Pattabiraman, R. H. Lasseter, and T. M. Jahns, "CERTS microgrids with photovoltaic microsources and feeder flow control," *ECCE 2016 - IEEE Energy Convers. Congr. Expo. Proc.*, pp. 1–8, 2016, doi: 10.1109/ECCE.2016.7854910.

[11]   P. Kotsampopoulos *et al.*, "A Benchmark System for Hardware-in-the-Loop Testing of Distributed Energy Resources," *IEEE Power Energy Technol. Syst. J.*, vol. 5, no. 3, pp. 94–103, 2018, doi: 10.1109/jpets.2018.2861559.

[12]   R. W. Erickson, *Fundamentals of Power Electronics*. Boston, MA: Springer US, 1997.

[13]   J. Rocabert, A. Luna, F. Blaabjerg, and P. Rodríguez, "Control of Power Converters in AC Microgrids," *IEEE Trans. Power Electron.*, vol. 27, no. 11, pp. 4734–4749, Nov. 2012, doi: 10.1109/TPEL.2012.2199334.

[14]   A. Yazdani and P. P. Dash, "A control methodology and characterization of dynamics for a photovoltaic (PV) system interfaced with a distribution network," *IEEE Trans. Power Deliv.*, vol. 24, no. 3, pp. 1538–1551, 2009, doi: 10.1109/TPWRD.2009.2016632.

[15]   L. Huang, H. Xin, Z. Wang, L. Zhang, K. Wu, and J. Hu, "Transient Stability Analysis and Control Design of Droop-Controlled Voltage Source Converters Considering Current Limitation," *IEEE Trans. Smart Grid*, vol. 10, no. 1, pp. 578–591, 2019, doi: 10.1109/TSG.2017.2749259.

[16]   M. B. Delghavi and A. Yazdani, "A control strategy for islanded operation of a distributed resource (DR) unit," *2009 IEEE Power Energy Soc. Gen. Meet. PES '09*, pp. 1–8, 2009, doi: 10.1109/PES.2009.5275592.

[17]   W. Yao, M. Chen, J. Matas, J. M. Guerrero, and Z. M. Qian, "Design and analysis of the droop control method for parallel inverters considering the impact of the complex impedance on the power sharing," *IEEE Trans. Ind. Electron.*, vol. 58, no. 2, pp. 576–588, 2011, doi: 10.1109/TIE.2010.2046001.